Mechanisms of Toxicity of Amorphous Silica Nanoparticles on Human Lung Submucosal Cells in Vitro: Protective Effects of Fisetin

ARTICLE *in* CHEMICAL RESEARCH IN TOXICOLOGY · AUGUST 2012

Impact Factor: 3.53 · DOI: 10.1021/tx3002884 · Source: PubMed

4 AUTHORS:

Joanna Mccarthy
Trinity College Dublin
8 PUBLICATIONS **108** CITATIONS
SEE PROFILE

Iwona Inkielewicz-Stepniak
Medical University of Gdansk
26 PUBLICATIONS **378** CITATIONS
SEE PROFILE

J. Jose Corbalan
Rutgers New Jersey Medical School
14 PUBLICATIONS **171** CITATIONS
SEE PROFILE

Marek Witold Radomski
Trinity College Dublin
243 PUBLICATIONS **14,874** CITATIONS
SEE PROFILE

Chemical Research in Toxicology

Article

pubs.acs.org/crt

Mechanisms of Toxicity of Amorphous Silica Nanoparticles on Human Lung Submucosal Cells in Vitro: Protective Effects of Fisetin

Joanna McCarthy,*[,†] Iwona Inkielewicz-Stępniak,[‡] J. Jose Corbalan,[†,§] and Marek W. Radomski[†]

[†]School of Pharmacy and Pharmaceutical Sciences, Trinity College, Dublin, Ireland

[‡]Department of Medicinal Chemistry, Gdansk Medical University, Poland

[§]Department of Chemistry and Biochemistry, Ohio University, Athens, Ohio 45701-2979, United States

ABSTRACT: There is growing evidence that amorphous silica nanoparticles (SiO_2-NP) can cause an inflammatory response in the lung. We studied in vitro the effects of exposing human lung submucosal cells to SiO_2-NP of various sizes (10, 150, and 500 nm) for 2−24 h. Cell survival, reactive oxygen species (ROS), malondialdehyde (MDA) levels, cytokine production, inflammatory gene expression, and genotoxicity were measured after exposure of Calu-3 cells to $10SiO_2$-NP in the presence or absence of the flavanoid fisetin and an antioxidant enzyme catalase. The exposure of Calu-3 cells to $10SiO_2$-NP resulted in (1) increased cytotoxicity and cell death in a time- and concentration-dependent manner, with a lethal concentration (LC_{50}) of 9.7 μg/mL after 24 h; (2) enhanced gene expression of interleukin (IL)-6, IL-8, and matrix metalloproteinase-9; (3) a significant correlation between increases in MDA and cytotoxicity at 18 h; (4) ROS production; (5) IL-6 and IL-8 release; and (6) up-regulation of the pro-apoptotic genes, p53 and caspase-3. Cell death and inflammatory reactions were attenuated by fisetin and catalase. We observed that 150- and $500SiO_2$-NP exerted no toxic effects on Calu-3 cells. In conclusion, the nanotoxicity of amorphous $10SiO_2$-NP on submucosal cells is associated with inflammation, the release of ROS leading to apoptosis, and decreased cell survival. The nanotoxic effects of $10SiO_2$-NP can be decreased by fisetin and catalase treatment, implicating oxidative stress in this injury.

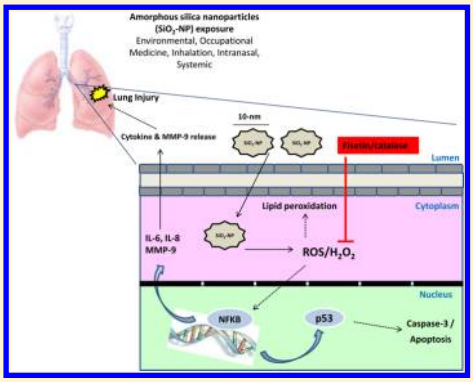

INTRODUCTION

The lung is one of the key targets for the possible toxic effects of nanoparticles as a result of environmental, occupational, or medicinal exposure.[1] Silicon dioxide or silica exists as crystalline or noncrystalline (amorphous) forms. It is well-known that exposure to crystalline silica is linked to pulmonary diseases such as silicosis.[2] There is a growing body of evidence that amorphous silica nanoparticles (SiO_2-NP) can cause toxic effects and inflammation in lung cells due to their unique physiochemical profile coupled with a size in the nanometer range.[3] Amorphous silica is used in many applications including diagnostic devices technologies and as therapeutic drug delivery systems.[4,5] Also, colloidal amorphous silica is widely reported to be used in metal casting, refractory products, and as a filter aid in food production.[6]

We investigated the effects of exposure of human lung bronchial submucosal cells, Calu-3, to engineered amorphous SiO_2-NP of various sizes; 10 ($10SiO_2$-NP), 150 (150SiO2-NP), and 500 nm ($500SiO_2$-NP). Most studies to date investigating the effect of SiO_2-NP in the lungs have been focused on human bronchial or alveolar cells.[7−9] However, within the respiratory system, epithelial cells in submucosal glands are involved in many important functions including maintenance of the viscosity and depth of the airway surface layer, which is a vital component of the lungs innate immune response against foreign bodies.[10] Furthermore, submucosal epithelial cells also express and secrete many markers and mediators of inflammation such as the pro-inflammatory cytokine interleukin-8 (IL-8), the pleiotropic cytokine IL-6, and matrix metalloproteinase-9 (MMP-9).[11,12] MMPs have been shown to interact with chloride ion channels on submucosal cells and thus can indirectly affect lung physiological processes associated with ion transport.[13]

There is also increasing research to suggest that engineered nanoparticles can exert profound effects in the lung. We have recently shown that polystyrene nanoparticles can affect cell signaling systems (Ca^{2+} and cAMP) controlling physiological processes on Calu-3 submucosal cells, specifically Cystic Fibrosis Transmembrane Regulator (CFTR) Cl^- ion channels.[14] Furthermore, Kasper and colleagues found that the apical exposure of amorphous SiO_2-NP to epithelial cells in an "epithelial-endothelial cells co-culture" induced the release of IL-8 and IL-6 to the basolateral side by both cell lines.[15] Besides this, SiO_2-NP have been shown to induce oxidative stress and apoptosis.[16−18] Importantly, both endothelial and bronchial epithelial cells are main targets for ingested and inhaled engineered nanoparticles, respectively, and thus play crucial roles in maintaining healthy physiological processes within the cardiovascular and respiratory systems.[19]

Received: June 26, 2012
Published: August 29, 2012

dx.doi.org/10.1021/tx3002884 | *Chem. Res. Toxicol.* 2012, 25, 2227−2235

We have recently proposed a mechanism for amorphous SiO_2-NP-induced inflammatory and cytotoxic effects in endothelial cells resulting from an increase in reactive oxygen species (ROS) generation followed by the enhanced gene expression of IL-6, IL-8, and MMP-9 in a size-, time-, and concentration-dependent manner.[20] Therefore, we hypothesized that amorphous SiO_2-NP could affect the integrity of human lung submucosal cells. Our data show that $10SiO_2$-NP are highly toxic to lung submucosal cells in comparison to larger SiO_2-NP of the same composite material and that the mechanism of toxicity is largely dependent on ROS production and oxidative stress. Interestingly, the cytotoxic effects of $10SiO_2$-NP could be attenuated in the presence of fisetin, highlighting a potential pharmacological use of flavonoids in protection of SiO_2-NP-induced cell damage.

MATERIALS AND METHODS

Reagents. Amorphous SiO_2-NP (unmodified) of different sizes were purchased from Polysciences (Eppelheim, Germany). All other items were purchased from Sigma-Aldrich unless otherwise stated.

Characterization of SiO_2-NP. Size measurements of $10SiO_2$-NP, $150SiO_2$-NP, and $500SiO_2$-NP used in this study have previously been described by using transmission electron microscopy.[20] The ζ-potential for all SiO_2-NP particles tested was determined using a Zetasizer Nano ZS (Malvern Instruments, Malvern, United Kingdom). The ζ-potential and polydispersity were measured at 25 °C with three repeats per sample. The dispersant (ultrapure water) had a pH of 7.4. Measurements were conducted using a concentration of 100 μg/mL of particle. In other experiments, the size and ζ-potential of all SiO_2-NP were tested in serum-free (SF) medium at 37 °C, pH 7.4, and at a final concentration of 100 μg/mL. The settings for ζ-potential analyses were as follows: the dielectric constant of the dispersant was set at 78.5; viscosity, as for water, at 0.6844 cP; and refractive index at 1.440.

Cell Culture. A Calu-3 cell line was obtained from the American Type Culture Collection (ATCC-HBT-55) and maintained as a monolayer culture in T-75 cm^2 tissue culture flasks. The cells were grown in Dulbecco's modified Eagle's medium, 1 g/L a low glucose medium containing also 110 mg/L sodium pyruvate and supplemented with 10% fetal bovine serum, 6 μg/mL penicillin-G, and 10 μg/mL streptomycin. Cells were maintained at 37 °C in a humidified atmosphere of 95% O_2−5% CO_2. Confluent cells were detached enzymatically with trypsin-EDTA and subcultured into a new cell culture flask. The medium was replaced every 2 days. Test solutions of SiO_2-NP particles (10-, 150-, and $500SiO_2$-NP) were prepared in SF culture medium and dispersed for 20 min using a sonicator (Cole-Parmer, 8890-MTH) before use to prevent aggregation.

Cellular Morphology. The morphology of Calu-3 cells in the presence of SiO_2-NP was visualized by phase-contrast microscopy. Briefly, cells were seeded onto glass coverslips contained in six-well plates at a density of 5×10^5 cells per well in complete medium. Preconfluent cells were treated under SF conditions with either $10SiO_2$-NP (50 μg/mL) or $150SiO_2$-NP and $500SiO_2$-NP (100 μg/mL) for 6 h at 37 °C. Control cells were unexposed to SiO_2-NP. Next, cells were washed twice with DPBS and fixed in 4% *para*-formaldehyde for 5 min at 37 °C. Fixed cells were mounted onto cover slides using a mounting medium, and images were obtained using a light microscope at 100× magnification ($ALTRA_{20}$ microscopy and CellA Acquisition software, Olympus, Japan).

Intracellular ROS Production by Fluorescent Microscopy. The detection of ROS in $10SiO_2$-NP-treated cells was carried out using a fluorometric assay based on the intracellular oxidation of 5-(and -6)-carboxy-2′,7′-dichlorodihydrofluorescein diacetate (carboxy-H_2DCFDA) (Molecular Probes). Calu-3 cells were seeded onto six-well plates at a density of 5×10^5 cells per well in complete medium. The following day, cells were treated with $10SiO_2$-NP in SF medium at varying concentrations of 1, 5, 10, 25, and 50 μg/mL. After a treatment period of 1 or 2 h at 37 °C, Calu-3 cells were washed with SF medium and exposed to carboxy-H_2DCFDA (40 μM) for 30 min at 37 °C. Finally, cells were washed twice with SF medium and viewed with the aid of a fluorescent microscope (Olympus IX81, Hamburg, Germany) at excitation and emission wavelengths of 485 and 530 nm, respectively.

Intracellular ROS Measurements by Fluorescence Spectrophotometer. Briefly, Calu-3 cells were seeded into 12-well plates at a concentration of 1×10^5 cells/well. The following day, cells were treated with either $10SiO_2$-NP alone at concentrations of 10, 25, and 50 μg/mL or were pretreated for 1 h with either fisetin (80 μg/mL) or catalase (400 U/mL) before exposure to $10SiO_2$-NP at the above concentrations for a 24 h period. Control cells were not treated with $10SiO_2$-NP. Afterward, cells were collected and then incubated with 40 μM carboxy-H_2DCFDA (Molecular Probes) for 15 min to assess ROS-mediated oxidation of DCF-DA to the fluorescent compound 2,7-dichlorofluorescin (DCF). The fluorescence of oxidized DCF was measured on a plate reader (FLUOstar OPTIMA, BMG Labtech, Aylesbury, United Kingdom) at excitation and emission wavelengths of 485 and 530 nm, respectively. Finally, the effect $10SiO_2$-NP in SF medium without cells to produce ROS species was measured as described above.

Cell Viability. The cell viability was measured by MTT assay. Calu-3 cells were seeded in triplicate at a density of 10^4 cells/100 μL of cell culture medium into 96 wells.[14] The next day, Calu-3 cells were treated with $10SiO_2$-NP, $50SiO_2$-NP, and $500SiO_2$-NP under SF conditions at the following concentrations, 0, 5, 10, 25, 50, and 100 μg/mL, and time points, 2, 6, 18, and 24 h. In other experiments, fisetin (80 μg/mL) or catalase (400 U/mL) was added 1 h prior to treatment with higher concentrations of $10SiO_2$-NP. As the control, the effect of fisetin on Calu-3 cell viability was tested at increasing concentrations for 1 h. This assay evaluates mitochondrial activity (assesses cell growth and cell death) and is performed by adding a premixed optimized dye solution to culture wells. The absorbance was recorded at 570 nm (FLUOstar, Optima, BMG Labtech). Results from treatment groups were calculated as a percentage of control values (unexposed cells) according to the following equation: % cytotoxicity = (experimental $abs_{570\ nm}$ of exposed cells/$abs_{570\ nm}$ of unexposed cells) × 100.

Flow Cytometry of IL-6 and IL-8. Calu-3 cells were cultured in T-25 cm^2 flasks until confirmed to be 80% confluent by phase-contrast microscopy. Cells were then treated with SiO_2-NP (10-, 150-, and $500SiO_2$-NP) in SF medium at varying concentrations (10, 25, 50, and 100 μg/mL) for 24 h at 37 °C. Next, conditioned medium was collected, and samples were centrifuged for 5 min at 300 RCF to remove cellular debris. The concentration of protein in the samples was quantified using a Bradford protein assay. Next, a BD CBA Human Inflammation kit (Oxford, United Kingdom) was used to quantitatively measure IL-8 and IL-6 from conditioned medium collected from controls and SiO_2-NP-treated Calu-3 cells by BD FACSArray (BD, Biosciences, Oxford, United Kingdom) (Corbalan et al.[20]). Controls were cells unexposed to SiO_2-NP. Measurements were performed according to the supplier's recommendations, and data were analyzed using the BD FACSArray system software version 1.0.3.

Real-Time Quantitative Polymerase Chain Reaction of MMP-9, IL-8, IL-6, Caspase-3, and p53. Calu-3 cells were cultured in T-25 cm^2 flasks in complete medium until confirmed to be 80% confluent by phase-contrast microscopy. Cells were treated with SiO_2-NP (10-, 150-, and $500SiO_2$-NP) in SF medium at varying concentrations (10, 25, 50, and 100 μg/mL) for 18 h at 37 °C. Controls were cells unexposed to SiO_2-NP particles. In other experiments, Calu-3 cells were treated as described above except that fisetin (80 μg/mL) or catalase (400 U/mL) was preincubated for 1 h prior to addition of $10SiO_2$-NP. Following incubation of cells with SiO_2-NP, conditioned medium was aspirated, and the cells were washed twice with phosphate saline buffer. DNA-free RNA was isolated using the Ambion RiboPure kit (Huntingdon, United Kingdom) according to the supplier's recommendations. RNA quantity and purity were assessed spectrophotometrically (Nanodrop ND-1000, Labtech International, Ringmer, Sussex, United Kingdom). Thereafter, the RNA in each sample was reverse-transcribed by the Applied Biosystems High Capacity cDNA Reverse Transcription kit (Woolston, United Kingdom). Real-time PCR was performed in duplicate, with predesigned Applied Biosystems TaqMan Gene Expression Assays for MMP-9, IL-8, IL-6, caspase-3, p53, and 18S ribosomal ribonucleic acid along with Applied Biosystems TaqMan Universal PCR Master Mix. In all experiments, 18S ribosomal ribonucleic acid was used as an

internal control. Both reverse-transcription and real-time PCR reaction were performed using the Eppendorf Realplex^2 Mastercycler (Histon, Cambridge, United Kingdom) (Corbalan et al.[20]). The expression of each gene within each sample was normalized against 18S rRNA expression and expressed relative to the control sample using the formula $2^{-(\Delta\Delta Ct)}$, in which $\Delta\Delta Ct$ = (Ct mRNA − Ct 18S rRNA)sample − (Ct mRNA − Ct 18S rRNA)control sample.[21]

Lipid Peroxidation. Calu-3 cells were plated into 24-well plates at a density of 1.5×10^5 cells per well in complete medium. Preconfluent cells were then exposed to 10SiO_2-NP at varying concentrations (1, 5, 10, 25, and 50 μg/mL) under SF conditions for 18 h at 37 °C. Malondialdehyde (MDA), a measure of lipid peroxidation, was measured using an Oxiselect TBARS Assay kit (Cell Biolabs, Inc., Cambridge, United Kingdom) following the manufacturer's instructions. Fluorescent measurements were recorded on a plate reader (FLUOstar OPTIMA, BMG Labtech) at excitation and emission wavelengths of 485 and 530 nm, respectively. The concentration of MDA in test samples was calculated using MDA standards as reference. The concentration of MDA in SiO_2-NP-treated cells is presented as the fold increase of MDA production over the control (untreated cells).

Statistical Analysis. Cytotoxicity is expressed as a percentage of relative viability of treated cells when compared to controls. The lethal concentration, LC_{50}, was derived from the following equation: log(inhibitor) vs responses curve, with an equation: Y = bottom + (top − bottom)/(1 + $10^{(\text{Log } IC_{50}-X) \times \text{Hill slope}}$). All data are presented as group means ± SDs for n individual experiments. Statistical analysis of the mean difference between multiple groups was determined by one-way ANOVA followed by Kramer−Tukey post-tests, and between two groups by unpaired t test as appropriate. A P value of <0.05 is considered statistically significant. All statistical and correlation analyses were performed using GraphPad Prism (Version 5.00 for Windows, San Diego, CA).

Table 1. Characterization of SiO_2-NP Used in This Study[a]

	10SiO_2-NP	150SiO_2-NP	500SiO_2-NP
concn (mg/mL)[b]	50.0	100.0	100.0
polydispersity index[c]	0.260	0.0240.026	
particles per gram[d]	9.55×10^{17}	2.83×10^{14}	7.20×10^{12}
size (nm)			
TEM[d]	10.5 ± 0.2	148.2 ± 2.2	495.9 ± 5.9
SF medium	12.5 ± 0.32	154.6 ± 0.95	492 ± 5.68
ζ-potential (mV)			
ultrapure water	−43.4 ± 1.7	−38.4 ± 0.3	−39.3 ± 0.1
SF medium	−25 ± 0.45	−27.3 ± 2.55	−29.6 ± 0.78

[a]Nanoparticle properties (stock suspension concentration, size, surface charge, polydispersity, particles per gram). [b]As supplied by the manufacturer. [c]Measurement made in ultrapure water. [d]As reported by Corbalan et al.[20]

RESULTS

Characterization of SiO_2-NP. The SiO_2-NP used in this study were commercially acquired being composed of pure silicon dioxide that is nonporous in character. We have previously measured the diameter of these nanoparticles (in ultrapure water) on transmission electron micrographs using ImageJ software to ensure consistency with the commercial specifications.[20] As we reported, 10-, 150-, and 500SiO_2-NP have a size of 10.50 ± 0.19, 148.20 ± 2.19, and 495.90 ± 5.87 nm, respectively; these previous measurements do not differ significantly from our current measurements in SF medium using the Zetasizer Nano ZS. Our previous TEM analyses also showed that the larger particles with a size greater than 100 nm (150- and 500SiO_2-NP) had a spherical shape, while the shape of the smaller 10SiO_2-NP were less uniform and had an irregular shape.[20] Using the light scattering technique, we found that the ζ-potentials of all tested SiO_2-NP (10-, 150-, and 500SiO_2-NP) had a negative charge greater than −30 mV in ultrapure water. When the ζ-potentials of all of the SiO_2-NP used in this study were retested in SF medium, we found that the greatest reduction in negative charge was for 10SiO_2-NP, which dropped from −43.4 to −25 mV, whereas for 150SiO_2-NP and 500SiO_2-NP the negative charge reduced in the range of 10−11 mV. A summary of the physiochemical characteristics of all tested SiO_2-NP used in this study is described in Table 1.

Effects of SiO_2-NP on Calu-3 Cell Morphology. Epithelial cells were exposed to 10SiO_2-NP for 6 h, and morphological changes were examined using phase-contrast microscopy (100×). Significant morphological changes in Calu-3 cells were observed after exposure of Calu-3 to 10SiO_2-NP (50 μg/mL), and these were characterized by features such as cell shrinkage and irregular shapes (Figure 1B) as compared with control cells (Figure 1A). The phase-contrast micrographs were indicative of cell death induced by silica nanoparticles, because Calu-3 cells detached from the cell culture dish after particle exposure. In contrast, 150SiO_2-NP and 500SiO_2-NP both at a high concentration of 100 μg/mL did not cause any morphological changes on Calu-3 cells (data not shown).

Effects of SiO_2-NP on Oxidative Stress and Lipid Peroxidation. 10SiO_2-NP induced oxidative stress (Figure 2A,B) and lipid peroxidation (Figure 2C) in a concentration-dependent manner. As compared with the control cells and cells incubated for 1 h, the highest oxidation of the oxidation marker carboxy-H_2DCFDA was observed after 2 h of incubation of Calu-3 with 50 μg/mL of 10SiO_2-NP. No effect on ROS production by Calu-3 cells was observed after treatment with 150 and 500SiO_2-NP for 1 and 2 h (data not shown).

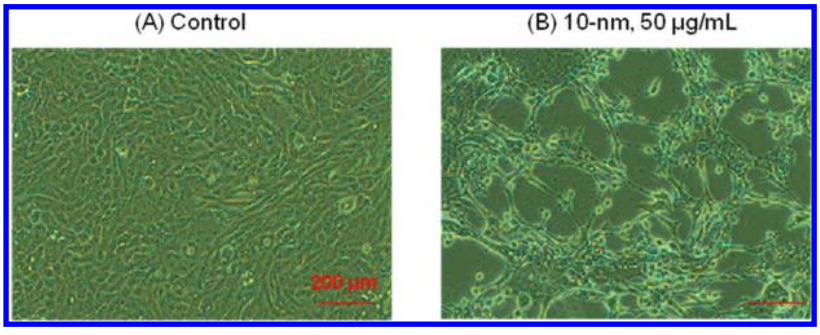

Figure 1. Morphological changes of Calu-3 cells exposed to 10SiO_2-NP for a period of 6 h followed by phase-contrast microscopy. Calu-3 cells exposed to 10SiO_2-NP 50 μg/mL (B) show cell death as compared with untreated cells (A) control (bar, 200 μm).

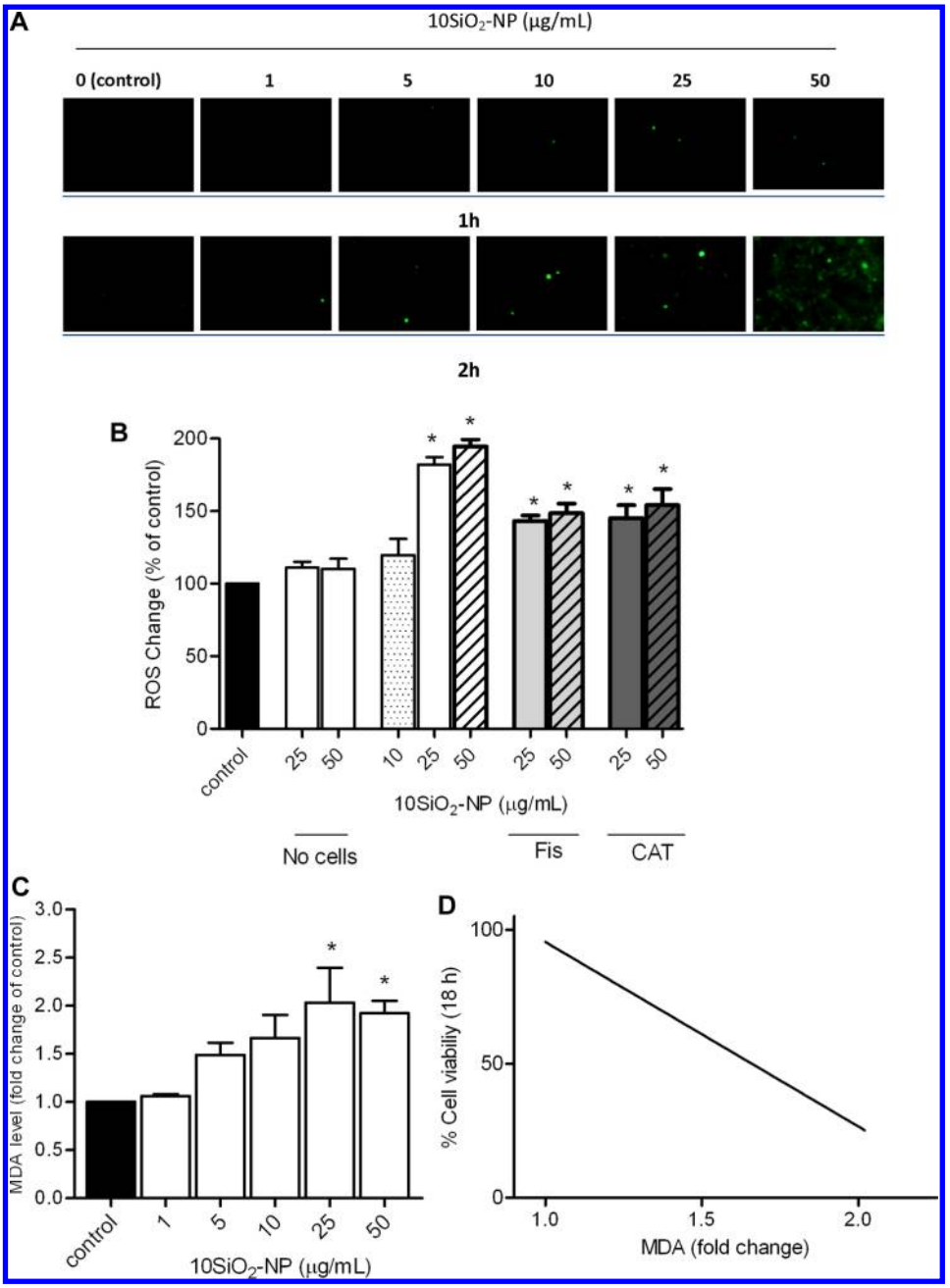

Figure 2. Induction of ROS and MDA by $10SiO_2$-NP in Calu-3 cells. (A) Calu-3 cells were exposed to $10SiO_2$-NP for either 1 or 2 h and incubated with carboxy-H_2DCFDA for 30 min at 37 °C. Cells were visualized by fluorescence microscopy (100×). (B) After 24 h, Calu-3 cells exposed to $10SiO_2$-NP produced significantly higher levels of ROS vs control cells (*P < 0.001, n = 3). Pretreatment of cells with fisetin (80 μg/mL) or catalase (400 U/mL) prior to exposure with $10SiO_2$-NP lead to a significant reduction in ROS production (*P < 0.001, n = 3). $10SiO_2$-NP without cells present did not produce ROS. (C) Cellular MDA levels in Calu-3 cells after prolonged exposure to $10SiO_2$-NP for 18 h. Control: 142.7 ± 18.2 nmol MDA/mg of total protein. *P < 0.05 vs control cells, n = 5. (D) Significant correlation between oxidant (MDA) and reduction in cell viability (MTT) in Calu-3 cells exposed to $10SiO_2$-NP for 18 h.

After 24 h, we found that Calu-3 cells exposed to $10SiO_2$-NP (25 and 50 μg/mL) produced significantly higher levels of ROS (182 ± 5.3 and 194.5 ± 6.8%, respectively) as compared to untreated cells (Figure 2B, *P < 0.05, n = 3). When cells were pretreated with fisetin (80 μg/mL) for 1 h prior to exposure with $10SiO_2$-NP (25 and 50 μg/mL), ROS production after 24 h was significantly reduced by 38.7 ± 3.8 and 46 ± 6.7%, respectively (Figure 2B, *P < 0.05, n = 3). Similarly, pretreatment of Calu-3 cells with catalase (400 U/mL) for 1 h also significantly reduced ROS production in $10SiO_2$-NP-treated cells at the same concentrations tested (Figure 2B, *P < 0.05, n = 3). In this case, ROS was reduced by 36.7 ± 8.7% in cells exposed to $10SiO_2$-NP at a concentration of 25 μg/mL and by 40 ± 11.2% in 50 μg/mL $10SiO_2$-NP-treated cells. Overall, fisetin and catalase pretreatment reduced ROS to comparable levels in $10SiO_2$-NP-treated cells after 24 h. However, each did not restore eliminate ROS production entirely or restore to control levels. $10SiO_2$-NP alone at a concentration of 25 and 50 μg/mL in the presence of medium only (i.e., without cells) did not produce any detectable ROS.

Lipid peroxidation is indicative of cellular damage. In turn, MDA is a natural biproduct of the lipid peroxidation process and

dx.doi.org/10.1021/tx3002884 | Chem. Res. Toxicol. 2012, 25, 2227−2235

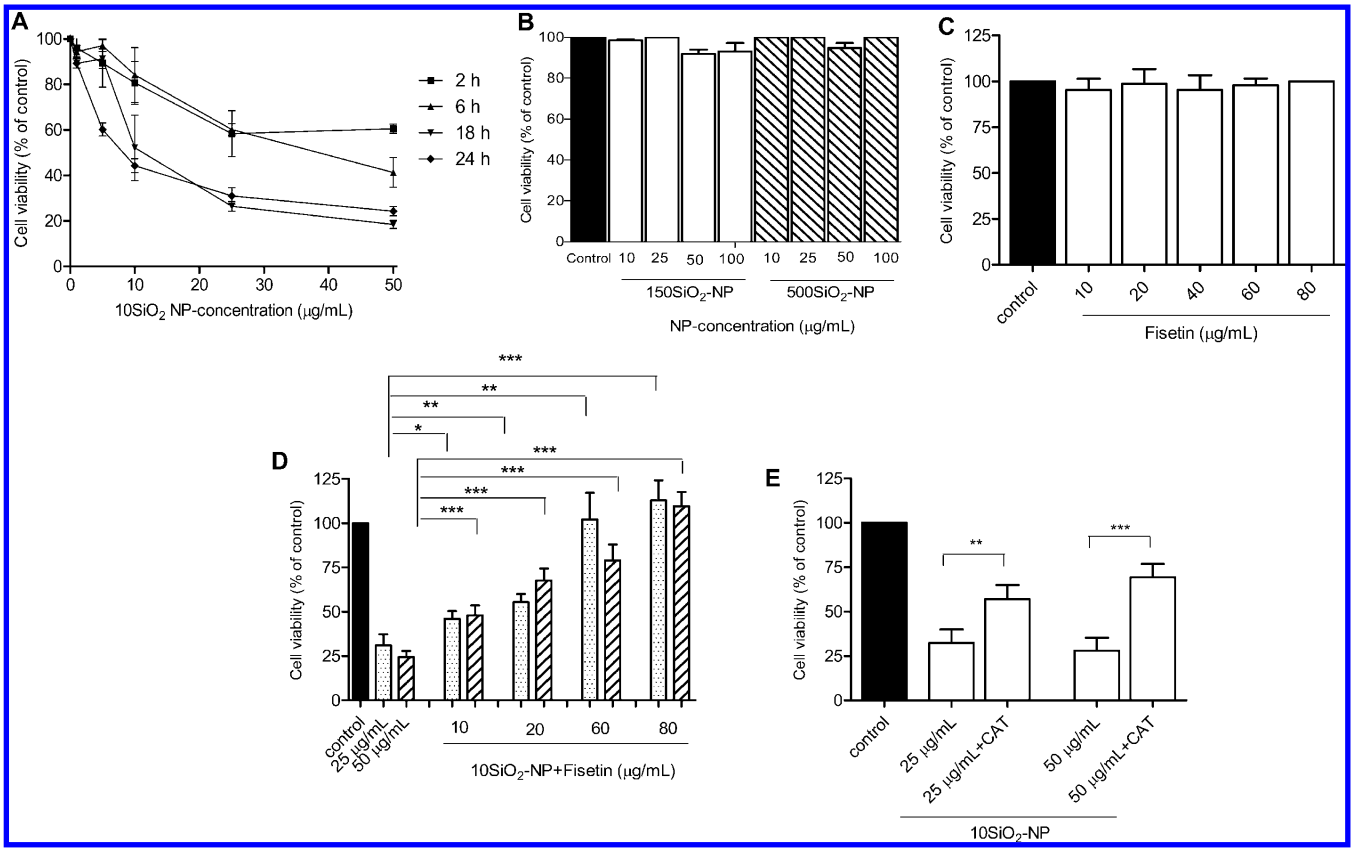

Figure 3. Effect of SiO_2-NP on Calu-3 cell viability. (A) Time- and concentration-dependent toxicity of $10SiO_2$-NP on Calu-3 cells. Cells were treated with $10SiO_2$-NP at varying concentrations (0−50 μg/mL) for 2, 6, 18, and 24 h. The cell viability was determined by MTT analysis at different time points. *$P < 0.05$ vs control cells, $n = 4$. (B) Viability of Calu-3 cells after prolonged exposure (up to 24 h) to increasing concentrations of 150- and $500SiO_2$-NP, $P > 0.05$ vs control cells, $n = 3$. (C) Fisetin at increasing concentrations (10−80 μg/mL) showed no significant cytotoxic effect on Calu-3 cell viability. (D and E) Prior incubation of cells with fisetin (D) and catalase (E) prevented the cell death induced by $10SiO_2$-NP (25 and 50 μg/mL) on Calu-3. *$P < 0.05$, **$P < 0.01$, and ***$P < 0.001$, $n = 3$−4.

thus is a marker for oxidative stress. Figure 2C shows that exposure of Calu-3 cells to increasing concentrations of $10SiO_2$-NP for an 18 h period increases MDA production. $10SiO_2$-NP at concentrations of 25 and 50 μg/mL significantly increased MDA production 2.03 ± 0.36- and 1.92 ± 0.13-fold, respectively, as compared to control (Figure 2C, *$P < 0.05$, $n = 5$). A significant linear regression ($R^2 = 0.97$) was found between increases in MDA oxidant levels and a reduction in cell viability in Calu-3 cells exposed to $10SiO_2$-NP for 18 h (Figure 2D, *$P < 0.01$).

Effect of SiO_2-NP on Cell Survival and Its Modulation by Fisetin and Catalase. Cells were exposed to $10SiO_2$-NP at concentrations up to 50 μg/mL for 2 or 24 h, and cytotoxicity was determined by cell viability assay. $10SiO_2$-NP were found to cause cytotoxicity on Calu-3 cells in a time- and concentration-dependent manner (Figure 3A, *$P < 0.05$). At 24 h, the cell viability was significantly decreased (*$P < 0.05$, $n = 4$) to 44.3 ± 3.06, 31.0 ± 3.6, and 24.3 ± 2.0% at the highest concentrations of $10SiO_2$-NP tested (10, 25, and 50 μg/mL, respectively). A fit (nonlinear regression) of the concentration−response curve at 24 h yielded a LC_{50} value of 9.7 μg/mL with a corresponding Hill coefficient of −0.92 ± 0.15. Larger nanoparticles ($150SiO_2$-NP and $500SiO_2$-NP) were not found to be cytotoxic to Calu-3 cells, even when tested at concentrations of 100 μg/mL for 24 h (Figure 3B). In another set of experiments, Calu-3 cells were exposed to $10SiO_2$-NP at concentrations of either 25 or 50 μg/mL in the presence or absence of fisetin (10−80 μg/mL) for 24 h. After treatment, cytotoxicity was determined by cell viability assay. It was found that fisetin attenuated the effects of 10 SiO_2-NP on Calu-3 cell viability (Figure 3D, *$P < 0.05$, $n = 3$), and this effect was maximal at 80 μg/mL. For control, the effect of fisetin alone on Calu-3 cell viability was tested at increasing concentrations (10−80 μg/mL) and was found to have no significant cytotoxic effect on Calu-3 cell viability or to interfere with the redox activity of the MTT assay (Figure 3B, $P > 0.05$, $n = 3$). Fisetin at a concentration of 80 μg/mL was used in subsequent experiments. Figure 3E shows that a $10SiO_2$-NP-induced decrease in cell viability was also attenuated by catalase.

Effect of SiO_2-NP on Inflammatory Gene Expression and Cytokine Release: Modulation by Fisetin and Catalase. The IL-6 gene expression was significantly up-regulated (fold change) by 15.9 ± 4.7 and 18.9 ± 1.2 in the presence of 25 and 50 μg/mL $10SiO_2$-NP, respectively (Figure 4A, *$P < 0.05$, $n = 3$−4). In contrast, 150- and $500SiO_2$-NP did not significantly increase IL-6 gene expression at all concentrations tested (25, 50, and 100 μg/mL) (Figure 4A, $P > 0.05$, $n = 3$−4).

Similar to IL-6, the gene expression of IL-8 was increased by $10SiO_2$-NP (Figure 4B). Again, $150SiO_2$-NP and $500SiO_2$-NP were found not to effect IL-8 gene expression at all concentrations tested (Figure 4B, $P > 0.05$, $n = 3$). The release of IL-6 and IL-8 proteins followed the gene expression pattern (Figure 4C,D). Finally, MMP-9 gene expression was significantly increased in response to $10SiO_2$-NP, an effect undetectable with 150- and $500SiO_2$-NP (Figure 4E, *$P < 0.05$, $n = 3$).

dx.doi.org/10.1021/tx3002884 | Chem. Res. Toxicol. 2012, 25, 2227−2235

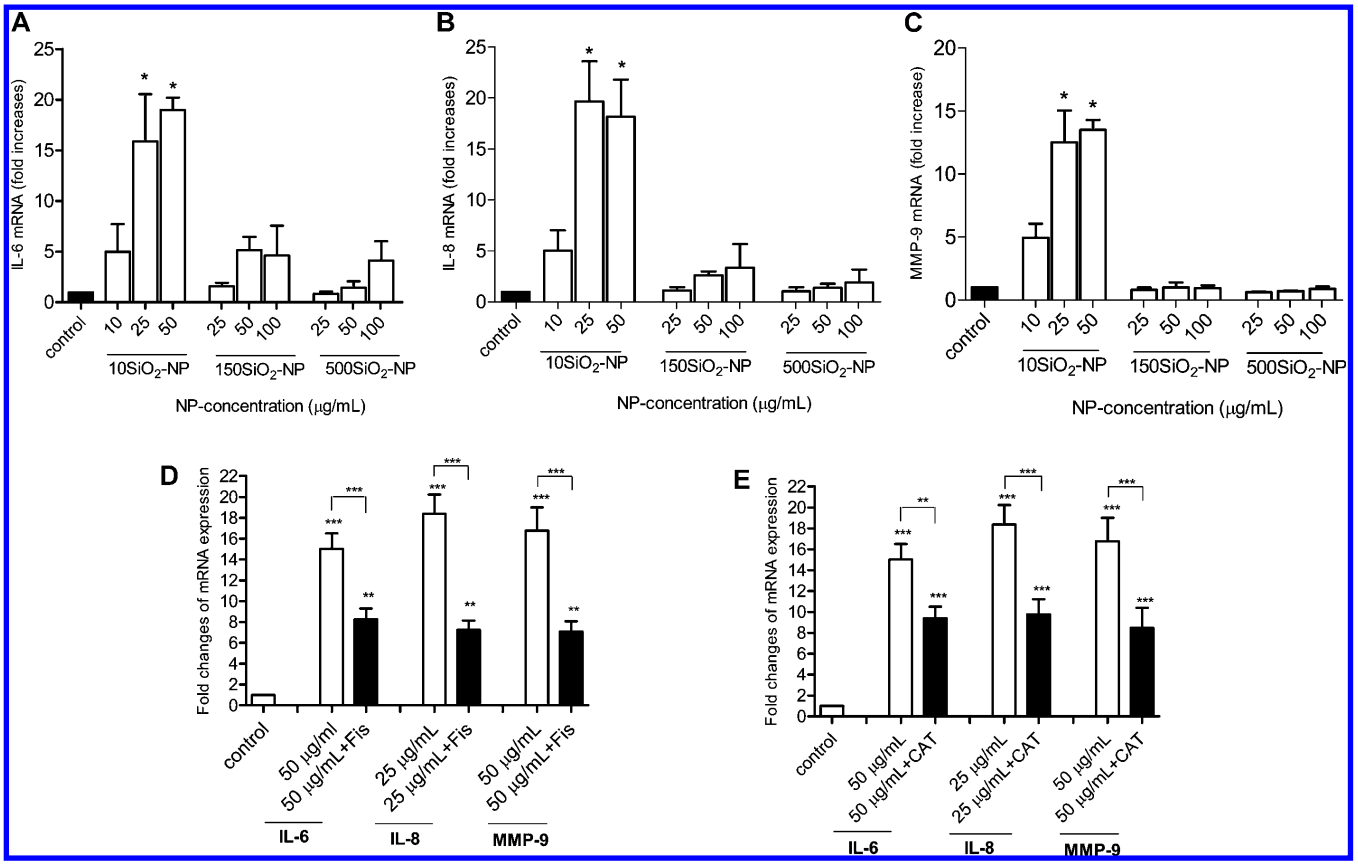

Figure 4. Effect of SiO_2-NP on the gene expression level of inflammatory markers in Calu-3 cells. Cells were treated with either 10-, 150-, and 500SiO_2-NP at varying concentrations (10, 25, 50, and 100 μg/mL) for 18 h. The gene expression of (A) IL-6, (B) IL-8, and (C) MMP-9 was investigated and found to be significantly up-regulated in 10SiO_2-NP-treated cells. *$P < 0.05$ vs control cells, $n = 4$. Prior incubation with fisetin (D) and catalase (E) prevented 10SiO_2-NP-induced up-regulation of IL-6, IL-8, and MMP-9 mRNA expression in Calu-3 cells. **$P < 0.01$ and ***$P < 0.001$, $n = 3$–4; treatments vs control cells. SiO_2-NP (25 and 50 μg/mL), fisetin (80 μg/mL), and catalase (400 U/mL)-treated cells in the absence or present of fisetin/catalase.

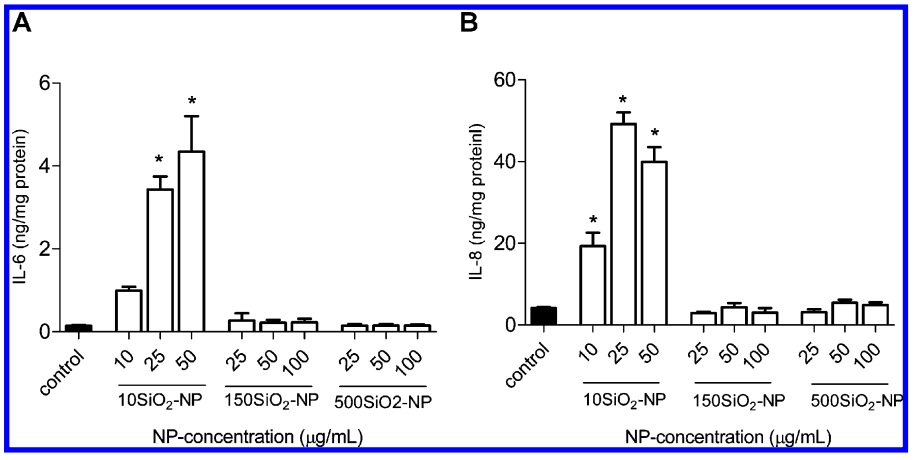

Figure 5. Effect of SiO_2-NP on cytokine release from Calu-3 cells. Cells were treated with 10-, 150-, and 500SiO_2-NP at varying concentrations (10, 25, 50, and 100 μg/mL) for 24 h. Both supernatants from control and SiO_2-NP treated cells were compared for the release of inflammatory cytokines IL-6 (A) and IL-8 (B) by flow cytometry. *$P < 0.05$ vs control cells, $n = 4$.

Pretreatment of Calu-3 cells with fisetin lead to a significant reduction in the inflammatory response of cells to 10SiO_2-NP, resulting in decreased expression of IL-6, IL-8, and MMP-9 mRNAs (Figure 5A). Similar to fisetin, pretreatment of Calu-3 cells with catalase significantly reduced the gene expression of IL-6, MMP-9, and IL-8 in response to 10SiO_2-NP (Figure 5B).

Stimulation of Apoptotic Markers by 10SiO_2-NP and Its Prevention by Fisetin and Catalase. The effects of 10SiO_2-NP on apoptosis were followed by measuring the expression of pro-apoptotic genes p53 and caspase-3. The treatment of cells with 10SiO_2-NP led to increased expression of p53 (Figure 6A) and caspase-3 (Figure 6B). These effects were attenuated by fisetin and catalase (Figure 6A,B, *$P < 0.05$, $n = 3$).

dx.doi.org/10.1021/tx3002884 | Chem. Res. Toxicol. 2012, 25, 2227–2235

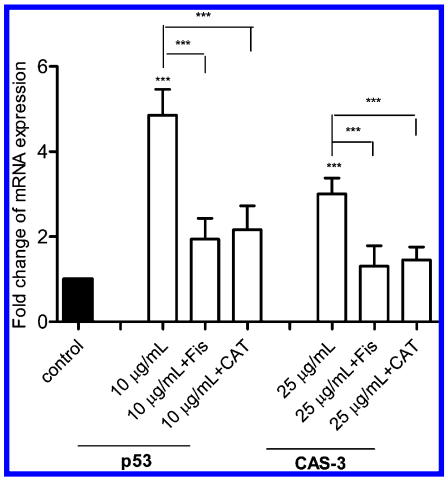

Figure 6. Effect of $10SiO_2$-NP on the gene expression of apoptotic markers in Calu-3 cells. Incubation of Calu-3 cells with fisetin or catalase avoided $10SiO_2$-NP-induced expression of p53 and CAS-3 mRNA. $^*P < 0.05$ and $^{***}P < 0.001$, $n = 3–4$; treatments as compared with control or as indicated. SiO_2-NP (10 and 25 μg/mL), fisetin (80 μg/mL), and catalase (400 U/mL)-treated cells in the absence or presence of fisetin/catalase.

DISCUSSION

This study has demonstrated that amorphous SiO_2-NP have the ability to decrease cell viability and induce cytotoxicity in human lung submucosal cells in a concentration- and size-dependent manner. Previous research studies have shown that SiO_2-NP with a size less than 100 nm are cytotoxic for cells. Lin et al. showed that the treatment of human broncho-alveolar A549 cells in vitro, to either 15 or 46 nm SiO_2-NP for 48 h at concentrations between 10 and 100 μg/mL, decreased cell viability in a concentration-dependent manner.[7] The cell viability of these A549 cells when exposed to 15 nm SiO_2-NP decreased to 68.1% at the highest concentration tested (100 μg/mL). In our study, we found that Calu-3 cell viability was reduced to 24.3 ± 2.0% when exposed to $10SiO_2$-NP for 24 h at a concentration of 50 μg/mL.

Napierska et al. showed in human endothelial cells that monodispersed SiO_2-NP caused cytotoxic cell damage and decreased cell survival in a concentration-dependent manner.[22] SiO_2-NP with sizes of 14, 15, and 16 nm had LC_{50} values ranging from 33 to 47 μg/cm^2 as compared to larger SiO_2-NP formulations of 104 and 335 nm, which exhibited lower cytotoxicity (LC_{50} of 1095–1087 μg/cm^2, respectively). Likewise, Gong et al. investigated the hazardous effects of SiO_2-NP (15, 30, and 100 nm) on human epidermal keratinocyte (HaCaT) cells in vitro. Their results show a similar trend as seen in our study with size-dependent nanotoxicity. In fact, 15 nm SiO_2-NP had a LC_{50} after 24 h of 19.4 ± 1.3 μg/mL.[23]

Rabolli et al. have shown in macrophage and fibroblast cells that nanoparticle surface area and not the aggregation state of the SiO_2-NP is a significant determinant for nanotoxicity.[24] Our own experiments show that small (10 nm) but not larger (150 or 500 nm) SiO_2-NP are cytotoxic to cells; thus, we support this proposal. Indeed, the increased surface area to mass ratio for the $10SiO_2$-NP as compared to 150- and $500SiO_2$-NP results in a greater percentage of atoms to be present at the surface of the silica nanoparticle, thus increasing the number of reactive groups at the particle surface that may influence toxicity.[1] In fact, a recent paper by Panas et al. showed that precoating 12 nm SiO_2-NP with serum proteins (fetal calf serum and bovine serum albumin) prevents the induction of toxicity and inflammation in A549 lung epithelial cells.[9]

Gong et al. showed that SiO_2-NP-induced cytotoxicity and DNA damage in HaCaT cells were dependent on ROS.[23] We have previously shown that amorphous $10SiO_2$-NP can induce rapid oxidative stress via ROS production in endothelial cells.[20] Here, we have demonstrated that $10SiO_2$-NP, but not larger ($150SiO_2$-NP and $500SiO_2$-NP), result in the intracellular ROS generation and lipid peroxidation in Calu-3 cells. The observed increases in MDA levels in Calu-3 cells were correlated with $10SiO_2$-NP cytotoxicity. Oxidative stress can activate the pro-inflammatory transcription factors AP-1 and NF-κB.[20,25,26] Studies with immortalized human endothelial cells have shown that lipid peroxidation induced by the cytokine TNF-α can result in NF-κB activation.[27]

In human bronchial airway epithelial cells, MAP kinases have been shown to regulate IL-8 promoter activity by NF-κB-dependent and -independent processes.[28] Singal and Finkelstein investigated the effects of 12 nm amorphous SiO_2-NP on mice alveolar epithelial cells.[29] By use of multiple MAP kinase inhibitors, they concluded that the transcription factor AP-1 was likely to play a role in amorphous SiO_2-NP-induced inflammatory gene up-regulation. Finally, we have found that selective inhibition of NF-κB with lactacystin attenuates downstream signaling triggered by $10SiO_2$-NP in the endothelium.[20]

This oxidative stress-induced transcription factor activation is likely to induce the cascade of inflammatory reactions. We have found that the treatment of lung submucosal cells with $10SiO_2$-NP leads to increased gene expression and release of IL-6, IL-8, and MMP-9. Studies have shown in vitro that the pro-inflammatory cytokines IL-6 can up-regulate MMP-9.[30] Inflammation-induced dysregulation of MMP-9, as shown by $10SiO_2$-NP in submucosal cells, could negatively impact normal physiological processes controlling ciliary beating, epithelial repair, and airway remodeling.

Studies by Ahmad et al. have shown that the naturally potent ROS scavenger vitamin C when cotreated with 15 nm SiO_2-NP on human liver cells can significantly attenuate the modulation of apoptotic markers (p53, bax, bcl-2, and caspase-3) and increase cell viability as compared to SiO_2-NP-only treated cells.[31] Thus, we wanted to investigate whether the nanotoxic effects of $10SiO_2$-NP could be pharmacologically attenuated using fisetin. Fisetin is a known bioactive plant flavanoid isolated at concentrations from 2 to 160 μg/g.[32] Flavonoids are diet-derived polyphenols that are increasingly used in health protection and therapeutics because of their remarkable cell-protective properties.[33,34] The mechanism of pharmacological action of these compounds may depend upon their antioxidant, free radical-scavenging ability including inhibition of superoxide, hydrogen peroxide (H_2O_2), and hydroxyl radical generation.[34]

We used fisetin at concentrations shown previously to be capable of preventing the cytotoxic effects of xenobiotics on hippocampal cells and bone osteoblast cells.[35] Interestingly, fisetin inhibited the nanotoxic effects of $10SiO_2$-NP by increasing cell viability, decreasing apoptotic markers, and reducing downstream generation of inflammatory mediators. Thus, our results with fisetin and $10SiO_2$-NP are in keeping with previously reported data by Ahmad et al. as described earlier using vitamin C.[31] The fact that fisetin only partially blocked the cytotoxic effects of $10SiO_2$-NP could be largely due to its low water solubility (<1 mg/g) and thus poor bioavailability in cell culture medium.[36] It is possible that the limited bioavailability of both fisetin and catalase in our experimental model could be due

dx.doi.org/10.1021/tx3002884 | Chem. Res. Toxicol. 2012, 25, 2227–2235

their nonspecific binding to $10SiO_2$-NP, otherwise known as the "protein corona" effect.[37]

As the effects described above with fisetin were mimicked by extracellular pretreatment with the catalase enzyme, it is likely that that the generation of H_2O_2 molecules plays a significant and major role in the nanotoxic effects of $10SiO_2$-NP on lung epithelial cells. In the cell, bioactive H_2O_2 is produced by superoxide dismutase from free oxygen radicals; these $1e^-$ or $2e^-$ oxygen molecules can come from the mitochondrial electron transport chain, lipooxygenase, cytochrome P450s, and other hemoproteins.[38] In turn, ROS/H_2O_2 can be generated in close proximity to the cell membrane, and if released outside of the cell, they can act in a paracrine fashion modulating cellular function.[39,40] The degradation of H_2O_2 involves intracellular catalase or extracellular glutathione. Our study indicates that there is an aberrant production of ROS by the lung submucosal cell in response to $10SiO_2$-NP exposure. A possible reason for the lack of complete removal of cytotoxicity to $10SiO_2$-NP by pretreatment with extracellular fisetin and catalase in Calu-3 cells could be related to the ongoing production and stimulation of ROS intracellularly. It is also possible that other non-ROS-mediated mechanisms are also involved in the cytotoxic effects of $10SiO_2$-NP.

CONCLUSION

Amorphous $10SiO_2$-NP can induce noxious effects in lung submucosal cells. Upon exposure of Calu-3 to $10SiO_2$-NP, cells rapidly produce ROS, which in turn causes lipid peroxidation. This oxidative stress can lead to an increase in transcription factor activation, and the subsequent up-regulation of cytokines (IL-6 and IL-8) and MMP-9 with eventual cytotoxicity, genotoxicity, and potential apoptosis via programmed cell death involving p53 and caspase-3. Importantly, all of these effects were detected in a size- and concentration-dependent manner and were preventable by pretreatment of lung cells with the flavonoid fisetin, thus highlighting the ability of these compounds to protect against the noxious effects of amorphous silica nanoparticles. Future toxicological studies examining the protection and thus relevance of fisetin in the in vivo situation would be worthwhile.

AUTHOR INFORMATION

Corresponding Author

*E-mail: mccartj7@tcd.ie.

Funding

This project was funded by a Science Foundation Ireland grant to M.W.R. and a Trinity College Dublin award to J.M. and J.J.C. I.I.-S. is on sabbatical leave from the Medical University of Gdansk.

Notes

The authors declare no competing financial interest.

ABBREVIATIONS

SiO_2-NP, amorphous silicon dioxide nanoparticles; SF, serum free; H_2O_2, hydrogen peroxide; ROS, reactive oxygen species; MMPs, matrix metalloproteinases; LC_{50}, lethal concentration; MDA, malondialdehyde

REFERENCES

(1) Card, J. W., Zeldin, D. C., Bonner, J. C., and Nestmann, E. R. (2008) Pulmonary applications and toxicity of engineered nanoparticles. *Am. J. Physiol. Lung Cell. Mol. Physiol. 295*, L400−411.

(2) Leung, C. C., Yu, I. T., and Chen, W. (2012) Silicosis. *Lancet 379*, 2008−2018.

(3) Napierska, D., Thomassen, L. C., Lison, D., Martens, J. A., and Hoet, P. H. (2010) The nanosilica hazard: Another variable entity. *Part. Fibre Toxicol. 7*, 39.

(4) Kumar, R., Roy, I., Ohulchanskky, T. Y., Vathy, L. A., Bergey, E. J., Sajjad, M., and Prasad, P. N. (2010) In vivo biodistribution and clearance studies using multimodal organically modified silica nanoparticles. *ACS Nano 4*, 699−708.

(5) Selvan, S. T., Tan, T. T., Yi, D. K., and Jana, N. R. (2010) Functional and multifunctional nanoparticles for bioimaging and biosensing. *Langmuir 26*, 11631−11641.

(6) Fruijtier-Pölloth, C. (2012) The toxicological mode of action and the safety of synthetic amorphous silica-a nanostructured material. *Toxicology 294*, 61−79.

(7) Lin, W, Huang, Y. W., Zhou, X. D., and Ma, Y. (2006) In vitro toxicity of silica nanoparticles in human lung cancer cells. *Toxicol. Appl. Pharmacol. 217*, 252−259.

(8) Eom, H. J., and Choi, J. (2009) Oxidative stress of silica nanoparticles in human bronchial epithelial cell, Beas-2B. *Toxicol. in Vitro 23*, 1326−1332.

(9) Panas, A., Marquardt, C., Nalcaci, O., Bockhorn, H., Baumann, W., Paur, H. R., Mülhopt, S., Diabaté, S., and Weiss, C. (2012) Screening of different metal oxide nanoparticles reveals selective toxicity And inflammatory potential of silica nanoparticles in lung epithelial cells and macrophages. *Nanotoxicology*, Epub ahead of print.

(10) McAuley, D. F., and Elborn, J. S. (2000) Cystic fibrosis: Basic science. *Paediatr. Respir. Rev. 1*, 93−100.

(11) Romano, M., Sironi, M., Toniatti, C., Polentarutti, N., Fruscella, P., Ghezzi, P., Faggioni, R., Luini, W., van Hinsbergh, V., Sozzani, S., Bussolino, F., Poli, V., Ciliberto, G., and Mantovani, A. (1997) Role of IL-6 and its soluble receptor in induction of chemokines and leukocyte recruitment. *Immunity 6*, 315−325.

(12) Greenlee, K. J., Werb, Z., and Kheradmand, F. (2007) Matrix Metalloproteinases in Lung: Multiple Multifarious and Multifaceted. *Physiol. Rev. 87*, 69−98.

(13) Duszyk, M., Shu, Y., Sawicki, G., Radomski, A., Man, S. F., and Radomski, M. W. (1999) Inhibition of matrix metalloproteinase MMP-2 activates chloride current in human airway epithelial cells. *Can. J. Physiol. Pharmacol. 77*, 529−535.

(14) McCarthy, J., Gong, X., Nahirney, D., Duszyk, M., and Radomski, M. (2011) Polystyrene nanoparticles activate ion transport in human airway epithelial cells. *Int. J. Nanomed. 6*, 1343−1356.

(15) Kasper, J., Hermanns, M. I., Bantz, C., Maskos, M., Stauber, R., Pohl, C., and Unger, R. E. (2011) Inflammatory and cytotoxic responses of an alveolar-capillary coculture model to silica nanoparticles: Comparison with conventional monocultures. *Part. Fibre Toxicol. 8*, 6.

(16) Wang, F., Gao, F., Lan, M., Yuan, H., Huang, Y., and Liu, J. (2009) Oxidative Stress contributes to silica nanoparticle-induced cytotoxicity in human embryonic kidney cells. *Toxicol. in Vitro 23*, 808−815.

(17) Xu, Z., Chou, L., and Sun, J. (2012) Effects of SiO(2) nanoparticles on HFL-I activating ROS-mediated apoptosis via p53 pathway. *J. Appl. Toxicol. 32*, 358−364.

(18) Ye, Y., Liu, J., Xu, J., Sun, L., Chen, M., and Lan, M. (2010) Nano-SiO2 induces apoptosis via activation of p53 and Bax mediated by oxidative stress in human hepatic cell line. *Toxicol. in Vitro 24*, 751−758.

(19) Medina, C., Santos-Martinez, M. J., Radomski, A., Corrigan, O. I., and Radomski, M. W. (2007) Nanoparticles: Pharmacological and toxicological significance. *Br. J. Pharmacol. 150*, 552−558.

(20) Corbalan, J. J., Medina, C., Jacoby, A., Malinski, T., and Radomski, M. W. (2011) Amorphous silica Nanoparticles trigger nitric oxide/peroxynitrite imbalance in human endothelial cells: Inflammatory and cytotoxic effects. *Int. J. Nanomed. 6*, 2821−2835.

(21) Livak, K. J., and Schmittgen, T. D. (2001) Analysis of relative gene expression data using real-time quantitative PCR and the 2(-Delta Delta C(T)) Method. *Methods 25*, 402−408.

(22) Napierska, D., Thomassen, L. C., Rabolli, V., Lison, D., Gonzalez, L., Kirsch-Volders, M., Martens, J. A., and Hoet, P. H. (2009) Size dependent cytotoxicity of monodisperse silica nanoparticles in Human endothelial cells. *Small 5*, 846−853.

(23) Gong, C., Tao, G., Yang, L., Liu, J., He, H., and Zhuang, Z. (2012) The role of reactive oxygen species in silicon dioxide nanoparticle-induced cytotoxicity and DNA damage in HaCaT cells. *Mol. Biol. Rep. 39*, 4915−4925.
(24) Rabolli, V., Thomassen, L. C., Uwambayinema, F., Martens, J. A., and Lison, D. (2011) The cytotoxic activity of amorphous silica nanoparticles is mainly influenced by surface area and not by aggregation. *Toxicol. Lett. 206*, 197−203.
(25) Chen, F., and Shi, X. (2002) NF-κB, a pivotal transcription factor in silica-induced diseases. *Mol. Cell. Biochem. 234−235*, 169−176.
(26) Liu, X., and Sun, J. (2010) Endothelial cells dysfunction induced by silica nanoparticles through oxidative stress via JNK/P53 and NF-KappaB pathways. *Biomaterials 31*, 8198−8209.
(27) Bowie, A. G., Moynagh, P. N., and O'Neill, L. A. (1997) Lipid peroxidation is involved in the activation of NF-kappaB by tumor necrosis factor but not interleukin-1 in the human endothelial cell line ECV304. Lack of involvement of H2O2 in NF-kappaB activation by either cytokine in both primary and transformed endothelial cells. *J. Biol. Chem. 272*, 25941−25950.
(28) Li, J., Kartha, S., Iasvovskaia, S., Tan, A., Bhat, R. K., Manaligod, J. M., Page, K., Brasier, A. R., and Hershenson, M. B. (2002) Regulation of human airway epithelial cell IL-8 expression by MAP kinases. *Am. J. Physiol. Lung Cell. Mol. Physiol. 283*, L690−699.
(29) Singal, M., and Finkelstein, J. N. (2005) Amorphous silica particles promote inflammatory gene expression through the redox sensitive transcription factor, AP-1, in alveolar epithelial cells. *Exp. Lung Res. 31*, 581−597.
(30) Kusano, K., Miyaura, C., Inada, M., Tamura, T., Ito, A., Nagase, H., Kamoi, K., and Suda, T. (1998) Regulation of Matrix Metalloproteinases (MMP-2, -3, -9, and -13) by Interleukin-1 and Interleukin-6 in Mouse Calvaria: Association of MMP Induction with Bone Resorption. *Endocrinology 139*, 1338−1345.
(31) Ahmad, J., Ahamed, M., Akhtar, M. J., Alrokayan, S. A., Siddiqui, M. A., Musarrat, J., and Al-Khedhairy, A. A. (2012) Apoptosis induction by silica nanoparticles mediated through reactive oxygen species in human liver cell line HepG2. *Toxicol. Appl. Pharmacol. 259*, 160−168.
(32) Kimira, M., Arai, Y., Shimoi, K., and Watanabe, S. (1998) Japanese intake of flavonoids and Isoflavonoids from foods. *J. Epidemiol. 8*, 168−175.
(33) Middleton, E., Jr., Kandaswami, C., and Theoharides, T. C. (2000) The effects of plant flavonoids on mammalian cells: implications for inflammation, heart disease, and cancer. *Pharmacol. Rev. 52*, 673−751.
(34) Goh, F. Y., Upton, N., Guan, S., Cheng, C., Shanmugam, M. K., Sethi, G., Leung, B. P., and Wong, W. S. (2012) Fisetin, a bioactive flavonol, attenuates allergic airway inflammation through negative regulation of NF-κB. *Eur. J. Pharmacol. 679*, 109−116.
(35) Inkielewicz-Stepniak, I., Radomski, M. W., and Wozniak, M. (2012) Fisetin prevents fluoride- and dexamethasone-induced oxidative damage in osteoblast and hippocampal cells. *Food Chem. Toxicol. 50*, 583−589.
(36) Ragelle, H., Crauste-Manciet, S., Seguin, J., Brossard, D., Scherman, D., Arnaud, P., and Chabot, G. G. (2012) Nanoemulsion formulation of fisetin improves bioavailability and antitumour activity in mice. *Int. J. Pharm. 427*, 452−459.
(37) Lundqvist, M., Stigler, J., Elia, G., Lynch, I., Cedervall, T., and Dawson, K. A. (2008) Nanoparticle size and surface properties determine the protein corona with possible implications for biological impacts. *Proc. Natl. Acad. Sci. U.S.A. 105*, 14265−14270.
(38) Cai, H. (2005) Hydrogen peroxide regulation of endothelial function: Origins, mechanisms, and consequences. *Cardiovasc. Res. 68*, 26−36.
(39) Alonso, D., and Radomski, M. W. (2005) Nitric oxide, platelet function, myocardial infarction and reperfusion therapies. *Heart Fail. Rev. 8*, 47−54.
(40) Rhee, S. G., Chang, T. S., Jeong, W., and Kang, D. (2010) Methods for detection and measurement of hydrogen peroxide inside and outside of cells. *Mol. Cells 29*, 539−549.